ELSEVIER

Polymer 42 (2001) 1633–1645

polymer

www.elsevier.nl/locate/polymer

Effects of molecular relaxation behavior on sized carbon fiber–vinyl ester matrix composite properties

K.N E. Verghese[a], R.E. Jensen[b], J.J. Lesko[a], T.C. Ward[b,*]

[a]*Department of Engineering Science and Mechanics, Virginia Polytechnic Institute and State University, Blacksburg, VA 24061, USA*
[b]*Department of Chemistry, Virginia Polytechnic Institute and State University, Blacksburg, VA 24061, USA*

Received 11 August 1999; received in revised form 25 April 2000; accepted 25 April 2000

Abstract

The mechanical and viscoelastic properties of unidirectional vinyl-ester carbon fiber composites were investigated. A cooperativity analysis of the composites was performed on storage (E') and loss modulus (E'') master curves obtained from dynamic mechanical analysis. The temperature sensitivity of the horizontal logarithmic shift factors ($\log a_T$), cooperativity, obtained from E' data, was found to vary with the sizing used to pretreat the carbon fibers. The observed variations in the experimental trends in cooperativity with fiber sizing for the composite materials were found to deviate significantly from theory. However, the trends in tensile and apparent shear strength of the composites matched the observed qualitative trends in viscoelastic cooperativity obtained from the storage modulus master curves. These results may suggest that the viscoelastic and ultimate mechanical properties of a composite material are related. However, several inconsistencies were observed when comparing the E'' and E' data which should also be considered in the interpretation of the experimental results.

Keywords: Cooperativity; Interphase; Short beam shear test

1. Background

An interphase may be defined in composites as a three-dimensional region that immediately surrounds the fiber and has attributes that differ from both the bulk matrix material and the fiber. This microscale interphase region, which often makes up less than 1 wt.% of the composite, has been shown experimentally by several authors to have a dramatic influence on performance [1–4]. The properties that are influenced range from tension, compression, toughness, fatigue and hygrothermal resistance. A comprehensive understanding of the composite interphase role in behavior is still lacking however. This is in part due to the several complexities involved. For example, polymer–polymer interdiffusion leads to a difficult graded material characterization problem. Additionally, a strong multidisciplinary approach to relate mechanical properties to molecular understanding is needed.

There have been many papers that interpret the properties of the fiber–matrix interphase of composite materials using data from dynamic mechanical analysis (DMA). Lewis and Nielsen [5] performed an early comprehensive study of an A-glass bead filled epoxy composite that is frequently cited. These researchers were primarily interested in determining the relative shear modulus of the filled epoxy composite in comparison to an unfilled epoxy control sample. It was observed that the relative shear modulus increased with increasing volume fraction of filler and decreasing particle size. The effect of increasing shear modulus was more pronounced in the rubbery response region at temperatures above the glass transition temperature (T_g). A slight temperature dependence of the relative shear modulus was also observed in the glassy region, but this was attributed to residual stresses due to a mismatch between the coefficients of thermal expansion for the glass filler and epoxy matrix.

In their study Lewis and Nielsen also examined the viscoelastic effects of pretreating the glass filler with different coupling agents. Methylchlorosilane (MCS) and γ-glycidoxypropyltriethoxysilane (GPS) were used to promote poor or good adhesion, respectively, between the filler and matrix epoxy. No noticeable effects of varying coupling agents were observed in the shear storage modulus curves. However, the shear loss modulus and damping ($\tan\delta$) curves varied significantly depending on the coupling agent that was used. The damping in the MCS case was greater than was found for the GPS pretreated

* Corresponding author. Tel.: 1-540-231-5876; fax: 1-540-231-8517.
E-mail addresses: kev@vt.edu (K.N.E. Verghese), tward@chemserver.chem.vt.edu (T.C. Ward).

0032-3861/01/$ - see front matter
PII: S0032-3861(00)00351-7

composite. The width of the tan δ curve was also wider for the GPS treated composite. Lewis and Neilsen believed that these changes in amplitude and width of the damping curves were caused by the specific interfacial interactions between the epoxy matrix and glass filler.

Cousin and Smith [6] observed changes in the tan δ curves of a sulfonated polystyrene ionomer that had been filled with small diameter alumina particles. The addition of the filler resulted in a broadening of the tan δ peak, as well as a decrease in the peak maximum amplitude, at the glass transition. They attributed the changes in the tan δ curves to the degree of the polymer–filler interactions occurring at this interface. Cousin and Smith also state that strong polymer–filler interactions will decrease the mobility and free volume of the polymer chains near the particle surface.

Eisenberg and Tsagaropoulos [7,8] theorized that two distinct regions of restricted mobility exist near the filler–polymer interface. The polymer chains nearest to the filler particle are tightly bound and are so highly restricted in mobility that they cannot participate in any transitions that are measurable by DMA. Beyond these tightly bound chains are loosely bound chains. There, they postulated chains that are more restricted in mobility when compared to the bulk polymer phase, but not as restricted as the tightly bound chains. If this model is correct then the differences in the damping curves of composite materials can be attributed to viscoelastic changes in the interphase region surrounding the filler particle. For example, a broadening in tan δ is predicted.

Reed [9] performed dynamic mechanical tests on glass–fiber reinforced epoxy matrix composites and observed a new thermal transition above the glass transition. Reed hypothesized that the existence of a resin region entrapped near the interface with a differing network structure was the cause for this higher temperature thermal transition. This additional transition also was detected as a change in the thermal coefficient of expansion for the composite.

Thomason [10] performed dynamic mechanical tests on several different composites comprised of glass fiber reinforced epoxy. Several different glass fibers with different sizing formulations were tested along with one carbon fiber composite. The appearance of the second transition at a temperature higher than the glass transition temperature was reported to exist only in the case of the glass fiber composites. Thomason attributed the second peak to be an artifact caused by a thermal lag caused during the heating of the sample at the specified heating rate, which results primarily from the low thermal conduction of the glass fibers. This second peak was shown to be dependant on the type of glass used, proportional to the amount of glass in the composite, orientation of the fibers and the heating rate. On a plot of peak temperature versus heating rate, it was shown that the position of the first peak did not change whereas the temperature increased linearly for the second peak. On the same plot, it was also seen that the second peak was non-existent for heating rates below 5°C/min. The glass transition for the clamped portion of the composite sample simply falls behind glass-to-rubber transition of the suspended portion between the DMA clamps, giving a second transition peak at a higher temperature. The argument low thermal conductivity of glass in composites was further supported by the disappearance of the second transition in the case of the carbon fiber specimens where there is a greater thermal conductivity. Thomason recommended therefore using heating rates below 5°C/min to prevent this problem. In the present case however the authors are only using carbon fiber composites and the heating rates are much lower than 5°C/min, eliminating the thermal gradient problem.

A broadening of the loss modulus and tan δ curves in composite materials when compared to neat resins can be credited to an increase in the breadth of the distribution of relaxation times (τ). Landel [11] observed these phenomena while studying the relaxation spectra of polyisobutylene that had been filled with glass beads. Fitzgerald et al. [12] considered the effects of the addition of a silicate network to the distribution of relaxation times in polyvinylacetate (PVAc). Fitzgerald et al. created dielectric loss master curves in the frequency domain for the PVAc/silicate composites. These master curves were then fitted to the Kohlrausch–Williams–Watts Eq. (1) to quantify the width of the distribution of relaxation times

$$\phi(t) = \exp\left[\left(\frac{t}{\tau}\right)^{(1-n)}\right] \tag{1}$$

In this equation (1) $\phi(t)$ is the Kohlrausch transient response function and n provides a measure of the width of the distribution of relaxation times [13]. When n is equal to 0 then the KWW equation describes the single relaxation time of a simple exponential decay [14]. In frequency space a simple Debye oscillator is imagined. However, the molecular environment of a polymer is much more complicated than the Debye model of simple rigid spheres, which are surrounded by a viscous fluid. Because of this complicated surrounding environment, polymers display a broad distribution of relaxation times. As n increases the breadth of the distribution of relaxation times also increases. This increase in the breadth of this distribution in relaxation times has also been attributed to an increase in the degree of coupling between polymer chains; hence n has also been referred to as a coupling parameter [15]. Fitzgerald et al. determined that the coupling parameter increased as more SiO_2 was incorporated into the PVAc. This was ascribed to the restriction of the mobility of the PVAc chains due to interactions with the silicate network.

Ngai and Roland [16] provided a molecular interpretation of cooperative motion. These researchers proposed that a relatively high level of intermolecular interactions increase the breadth of the distribution of relaxation times in a polymer. If a polymer segment could be isolated as a single unit then at $T = T_g$ this segment would have a unique relaxation

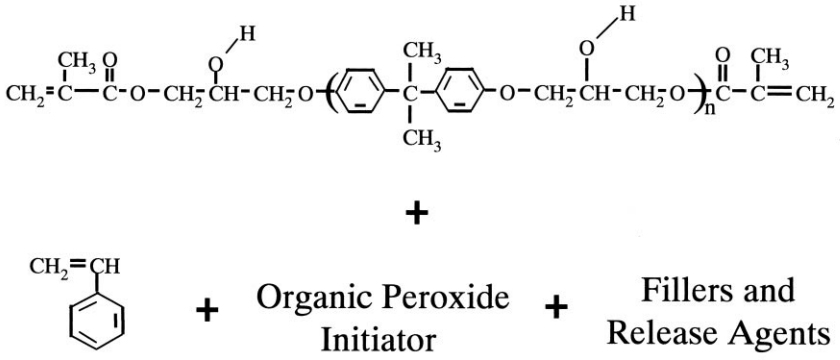

Fig. 1. Pultrudable vinyl-ester resin matrix used in graphite composites.

time. Under the dense conditions of the solid state the polymer is in close contact with neighboring chains. As thermal energy is raised, a segmental motion begins to occur at T_g and some of the segments cannot relax without involving non-bonded units in the vicinity. The constraining effect due to neighboring chains slows down the overall relaxation time depending on the volume of the cooperating unity. The coupled segmental relaxations of the polymer chains obviously do not occur at the same time or rate throughout the sample given the heterogeneity of all of the polymer parameters. This leads, phenomenologically, to an increase in the breadth of the distribution of relaxation times. A higher degree of intermolecular coupling and constraints from neighboring segments will increase the amount of cooperative segmental motion required in the transition from the glass to rubber [17]. In other words, the segmental motion of neighboring segments is correlated to a greater degree. Polymers with a high amount of cooperativity have viscoelastic properties that exhibit stonger temperature dependence of the time–temperature shift factors in the glass transition region.

The relative magnitude of the coupling parameter can then be determined by plotting the associated horizontal time–temperature shift factors ($\log a_T$) versus a temperature scale which has been normalized based on a fractional deviation from T_g. Plazek and Ngai [15] originally developed the following empirical expression (2) for determining the coupling parameter of bulk polymers using this type of analysis

$$(1 - n) \log a_T = \frac{-C_1(T - T_g)T_g}{C_2 + (T - T_g)/T_g} \quad (2)$$

This equation is similar in form to the Williams–Landel–Ferry (WLF) equation, except that temperature has been normalized by T_g and the coupling parameter is present. Plazek and Ngai determined that the C_1 and C_2 constants could be universally applied to a wide variety of bulk polymers, having values of 5.49 and 0.141, respectively. Experimental values of the coupling parameter n, which is the same constant as described by the KWW equation, have values that can range from 0.45 for polyisobutylene to 0.76 for polyvinylchloride [15]. Jensen et al. [18] used this method of analysis to model the viscoelastic response of epoxy/E-glass fiber composites. Their characterization technique required the generation of master curves using data acquired from dynamic mechanical analysis. Jensen et al. determined that the coupling parameter of an epoxy matrix increases significantly within this typical range upon the addition of E-glass fibers to the epoxy, but noted deviation from the predicted theory.

In summary of this introduction, dynamic mechanical analysis of composite materials has been used extensively to draw conclusions pertaining to the level of interaction between the matrix polymer and fiber reinforcement. The possibility of using DMA to gauge the response of the fiber–matrix interphase is desirable, as mechanical testing of composites is expensive and time consuming [19]. A common theory proposed by researchers studying the dynamic viscoelastic response of composite materials is that an elevated degree of molecular interaction between the fiber and matrix polymer will restrict the mobility of the polymer chains the interphase region near the fiber surface. Based on the assumption of reduced interfacial molecular mobility an analysis of cooperativity may hold the potential to yield a different viscoelastic perspective of a composite material than is offered by comparing the peak heights or widths of tan δ or E'' curves. Therefore, this paper will focus in detail about the possible applicability of cooperativity plots in characterizing the interfacial properties of composite materials. In doing so this will emphasize another goal of this work; to investigate a "non-destructive" experimental measure such as cooperativity to qualitatively understand an ultimate property such as strength.

2. Experimental

2.1. Materials and sample preparation

The matrix material for the composites was a pultrudable

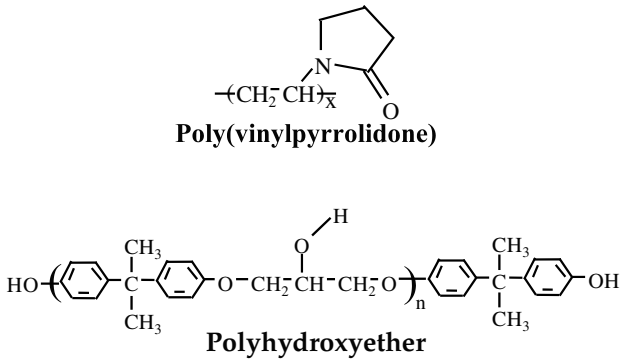

Fig. 2. Sizings used to pretreat the graphite fibers.

vinyl-ester (see Fig. 1) and the composites were all fabricated using the pultrusion processes. Hexcel AS-4 12K unsized carbon fiber (lot # D1317-4C) was sized at Virginia Tech with two different thermoplastic materials: a carboxylic acid poly(hydroxyether)-Phenoxy™ and a poly(vinylpyrrolidone)-K-90 PVP™ (see Fig. 2). The Phenoxy™ sizing material (PKHW-35 lot # 217013) was obtained from Phenoxy Associates, Rock Hill, SC. This material was obtained as a 35 wt.% dispersion of approximately 1 μm diameter particles in water. The M_n of the Phenoxy was 19,000 g/mol (GPC) and it had a T_g of 97°C (DSC). The K-90 PVP sizing material (LUVISKOL lot # 20421501) was obtained from BASF. The M_n of this material was 1,250,000 g/mol and it had a T_g of 180°C [20]. The K-90 PVP sized fiber had a diameter approximately equivalent to the high-spread Phenoxy. Hexcel AS-4 G' sized 36K fiber (lot # D1383-5K) was used as the control fiber for these trials and was provided by Strongwell Inc, who also conducted the pultrusion runs. The G' sizing present on this fiber has been considered the industrial benchmark sizing for the vinyl-ester matrix. Mechanical property data on the two fiber systems utilized in this studied clearly showed that no significant property difference existed between the two fiber lots.

The sized fiber was analyzed for sizing content and consistency using burn-off techniques. No analysis was performed on the commercial G' sized fiber. Pultrusion was performed at Strongwell using their lab scale pultruder and their standard pultrudable vinyl-ester resin (Derakane 411-35). The die utilized for this study had a cross-section of 0.5 in. × 0.075 in. The sized fiber spools were loaded into the creel rack and pulled through the resin dip bath. The same resin was utilized for all four pultrusion trials. The composite was then cured in the die. Details regarding the sizing process and the pultrusion of the fiber can be found in an earlier publication [21]. The fiber volume fraction of the composite panels produced in these experiments was determined by two methods [22]. The first method utilized data collected before the composite part was produced and was termed the theoretical fiber volume fraction. The second method utilized data collected after the composite part was produced and was termed the experimental fiber volume fraction.

For the first method, the number of tow ends and their respective linear density allowed the determination of the volume of fiber per unit length entering the pultrusion die. The fiber volume fraction could then be computed from the following equation

$$\nu_f = \frac{(n - l_f)}{(A_c \cdot \rho_f)} \tag{3}$$

where, ν_f is the fiber volume fraction, n the number of tow ends, l_f the weight per unit length per bundle, A_c the cross-sectional area of the composite, and ρ_f is the filament density. The cross-sectional area of the composite, A_c, was determined from the die cross-sectional area (neglecting matrix shrinkage) or from the final composite cross-sectional area (including matrix shrinkage). This method neglects the mass of fiber lost in the pre-processing portions of the pultrusion process, which is negligible in most cases. Using Eq. (3), the theoretical fiber volume fraction of the G'' composite was 65.6% and that for the thermoplastic sized composites were 61.1%.

For the second method, the density of the composite was determined and a rule of mixtures was used to determine the fiber volume fraction. A 4 g sample of the composite was dried and weighed. The sample was then immersed in isopropyl alcohol and weighed again. The density of the composite was calculated using Archimedes' principle using the following equation:

$$\rho_{composite} = W_{air}(W_{air} - W_{IPA})\rho IPA \tag{4}$$

where, $\rho_{composite}$ is the density of the composite, ρ_{IPA} the density of Isopropyl alcohol, W_{air} the weight of sample in air and W_{IPA} is the weight of sample in isopropyl alcohol. The fiber volume fraction was then calculated using the rule of mixtures

$$\nu = \frac{(\rho_{composite} - \rho f)}{(\rho_{resin})} \tag{5}$$

where, ν is the fiber volume fraction of the composite, $\rho_{composite}$ the density of the composite calculated from Eq. (4), ρ_f the density of the carbon fiber and ρ_{resin} is the density of the cured resin. Eq. (5) assumes that the composite has zero void volume. The difficulty in applying Eq. (5) is that the resin density, ρ_{resin}, is not known exactly. The fiber volume fractions using this method are as follows, 68.0 ± 0.3%, 65.0 ± 0.6%, 61.1 + 0.6%, and 6.39 + 0.2 composites, respectively. Ultrasonic C-scan measurements and cross sectional microscopy was also performed to ensure quality control. Details of the procedure can be found in Ref. [22].

2.2. Mechanical properties tests

Mechanical property tests included static tension, longitudinal flexure, and short beam shear (SBS). The quasi-static

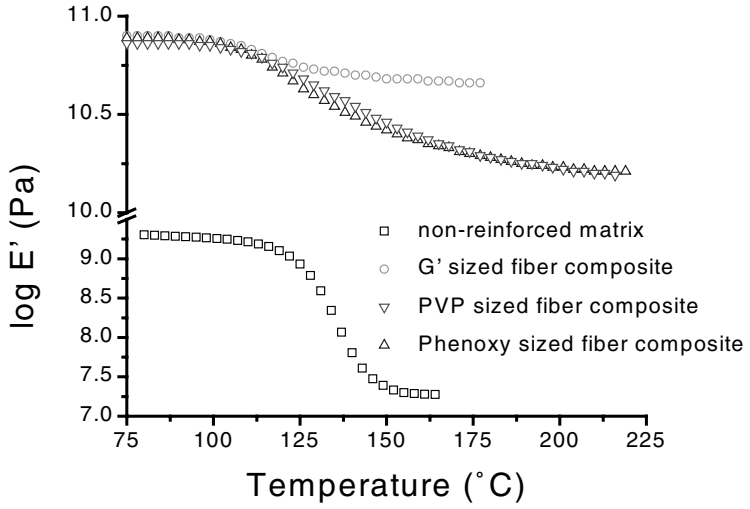

Fig. 3. Storage modulus curves for graphite composite samples as well as non-reinforced matrix versus temperature obtained from DMA (1 Hz).

tension tests were performed at room temperature on a servo-hydraulic MTS testing machine. The tests were conducted in load control at a loading rate of approximately 200 lb/s. The loading cycle was programmed into the Microplrofiler™. A MTS 448.82 test controller was used to control the machine once the test was started. Strain during the experiments was measured using a 1 in. gauge length, MTS Model 632 extensometer. The signal from the extensometer was conditioned using a 2310 Vishay Measurements Group amplifier box. The specimens were tabbed using a high-pressure laminated glass–epoxy material. This was done in order to prevent the unidirectional composite samples from crushing in the grips of the machine. The tabs were sand blasted and attached to the specimen using a 3 M, DP40 epoxy adhesive. The adhesive was cured in an oven at 50°C for 2 h. The grip pressure on the specimen was controlled at 7 MPa. The short beam shear tests were performed in accordance with ASTM D 2344-84, on a screw driven Instron 4104 test frame. The sample length was 11 mm in accordance with the length to thickness ratio for carbon fiber composites. The loading rate of 1.3 mm/min was used.

2.3. Dynamic mechanical tests

Dynamic mechanical analysis was performed using Du Pont instruments DMA 983 in flexural bending mode with an amplitude displacement of 0.20 mm peak to peak. The samples were cut with a Behuler Isomet saw using a diamond wafer blade. Typical clamped sample dimensions were $30.0 \times 12.8 \times 1.9\ \text{mm}^3$. The primary advantage of using the Du Pont DMA is that the clamp width can be optimized for very stiff composites. The clamp width of 30.0 mm yielded excellent results. The oscillation amplitude of the instrument was also varied to insure that the viscoelastic response of the samples was linear. The temperature was ramped from 80 to 220°C in 3°C increments under a nitrogen atmosphere. At each temperature

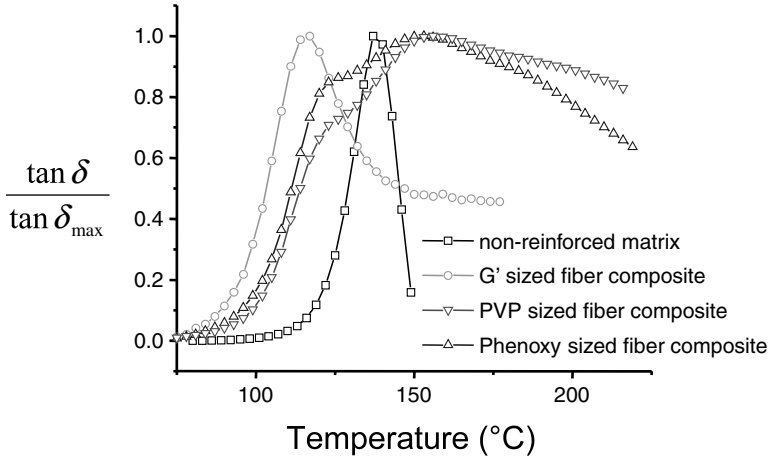

Fig. 4. Normalized tan δ curves obtained from DMA measurements (1 Hz).

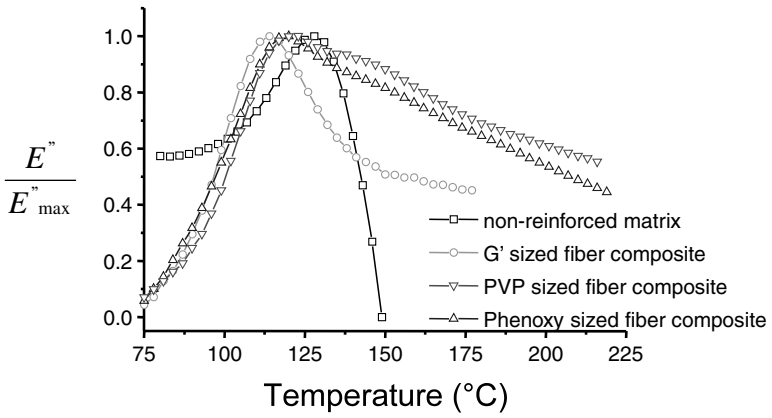

Fig. 5. Normalized E'' curves obtained from DMA measurements (1 Hz).

step the viscoelastic response of the composite was measured at frequencies of 0.03, 0.1, 0.3, 1, 3, and 10 Hz. On completion of the measurements at 220°C the composite specimen was allowed to slow cool to room temperature in the instrument and the measurement procedure was repeated. All of the data used for this paper was taken from the second heat measurements in the DMA. This insures that each sample has the same thermal history. A minimum of four samples were measured for each group of composite specimens.

3. Results and discussion

The dynamic E' curves obtained at 1 Hz for the composite samples and non-reinforced matrix are illustrated in Fig. 3. From this data it is readily apparent that the addition of the graphite fibers significantly increases the modulus of the matrix polymer. The glassy modulus is elevated from approximately $10^{9.5}$ Pa for the matrix to about $10^{10.8}$ Pa for the composites. The composite samples have similar glassy modulus values. The rubbery modulus is also much higher in the composites than in the non-reinforced matrix. The G' sizing yielded the highest rubbery modulus, while the Phenoxy and PVP sized fiber samples have similar values of rubbery modulus. The increased value of rubbery modulus for the G' sized fiber samples could be due to a slightly higher volume fraction of fibers. The glass-to-rubber transition regions of the composite samples are also much broader than in the non-reinforced matrix.

A closer examination of the glass-to-rubber transition of the composites and the non-reinforced matrix can be seen in the normalized tan δ and E'' curves (1 Hz) shown in Figs. 4 and 5, respectively. The matrix has the highest T_g (138°C), as defined by the peak maximum of the α-transition. This could probably be due to the absence of processing aids that are typically added in the pultrusion process, which could act as plasticizers in depressing the glass transition temperature, as well as differences in the thermal histories of the non-reinforced and fiber reinforced samples. The T_gs of the composite samples range from 116°C for the G' sized fiber sample to 122 and 125°C for the Phenoxy and PVP sized fiber samples respectively. The α-transition of the PVP and Phenoxy sized composite samples was taken as the low temperature shoulder that is present in the tan δ curves. Both the PVP and Phenoxy sized fiber composites exhibit a distinct second transition peak above 150°C. This is not due to a plasticizing of the matrix by the sizing as data obtained by Verghese [23] has shown that the tensile modulus of samples made by blending the sizing at different concentration into vinyl ester remains relatively constant. The fiber packing features of the different composites have also been shown to be relatively the same. The shoulders on the Phenoxy and PVP curves both occur near the same temperature as the α-transition peak of the G' curve. The higher temperature transitions evident in the Phenoxy and PVP sized fiber composites could be the glass transitions of the sizings themselves, or a highly restricted interphase region near the fiber surface. The higher temperature transitions evident in the tan δ curves were very consistent and reproducible. Thomason [10] published results which indicate that a high temperature peak in the loss modulus or tan δ curves of a fiber-reinforced composite could be an artifact of the DMA due to the thermal lag in the sample. However, in our case the measurement technique used for these experiments, the step-isothermal mode, precludes such a lag. Specifically, the DMA increases temperature in 3°C increments, equilibrates at the designated temperature, and then sweeps the assigned frequencies. The low frequency measurement (0.03 Hz) is responsible for making this step iso-thermal procedure much slower than a more common constant heating rate experiment. Total measurements (from 80 to 220°C) were typically completed overnight with 25–30 min required at each individual temperature step. Due to the lengthy step times that the composites experienced in the DMA, confidence can be placed in the judgement that the additional high temperature tan δ peaks in the Phenoxy and PVP samples are not artifacts.

The composite samples also have tan δ curves that are much broader than the non-reinforced matrix. This

Table 1
Summary of transition temperatures in non-reinforced matrix and fiber composite samples

Sample	T_g (α-transition) (°C)	$T_{\text{second transition}}$ (°C)
Non-reinforced matrix	138	Not present
G' sized fiber composite	116	Not present
PVP sized fiber composite	125	159
Phenoxy sized fiber composite	122	152

increased peak broadness and absence of the second transition in the E' curves is consistent with the findings of Lewis and Nielsen [5]. The transition temperatures obtained from the tan δ curves are summarized in Table 1.

3.1. E' master curves

The time–temperature superposition (time–temperature superposition) procedure was used to construct master curves of the storage modulus in the frequency domain for each of the samples studied. The glass transition temperatures, taken as the peak maximums of the tan δ curves at 1 Hz, were used as the reference isotherms. Master curves were successfully created from the storage modulus data. However, this was not the case for the loss modulus data, as will be discussed in the following section. The normalized E' master curves for the composite and non-reinforced matrix samples are depicted in Fig. 6. The composite sample master curves were slightly noisier, but highly reproducible. The fiber reinforcement extents the glass-to-rubber transition zone to much lower frequencies, or longer times, than the non-reinforced matrix. The Phenoxy sample extends to the lowest frequencies, followed by the PVP and G' and non-reinforced matrix samples, respectively.

3.2. E' cooperativity

Horizontal shift factor values were obtained from the generation of the E' master curves. Cooperativity plots

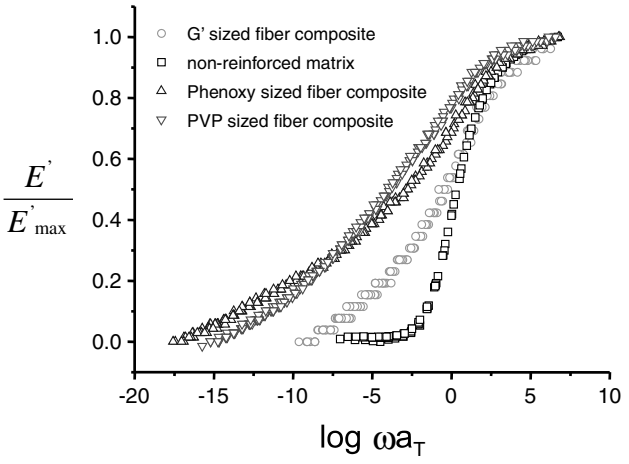

Fig. 6. Normalized E' master curves.

were then produced following the analysis of Plazek and Ngai [15]. The cooperativity plots are illustrated in Fig. 7. The cooperativity of the composite samples, based upon the E' data, clearly varies depending on the sizing that was used to pretreat the fibers. Again, these plots were very reproducible. At least four samples were measured for each sizing and the standard deviation is negligible compared to the absolute values. The $\log a_T$ values for the composite samples are found to have greater temperature dependencies at temperatures $T > T_g$ than the non-reinforced matrix, as illustrated in Fig. 7. The Phenoxy sized fiber composite shows the greatest temperature dependence, followed closely by the PVP sized sample. The shift factors for the G' samples have an intermediate temperature dependency between the matrix and the PVP sample. All of the composite samples exhibit similar non-equilibrium behavior in the glassy state, which is greater than the non-reinforced matrix sample.

Fig. 8 shows an expanded view of the cooperativity plots at $T > T_g$ for all of the samples. The curves have also been best fit to Eq. (2) using a non-linear regression. The analysis of Plazek and Ngai provides a reasonable description of the viscoelastic behavior of the non-reinforced matrix using the literature values for the constants C_1 and C_2. Eq. (2) does not accurately fit the cooperativity data of the composite materials. Eq. (2) predicts a WLF type curve that is concave up and that gradually levels off at $T \gg T_g$. While the $\log a_T$ values for the non-reinforced matrix begin to plateau at temperatures approximately 30°C greater than T_g, where $(T - T_g)/T_g \approx 0.05$, the $\log a_T$ values for the fiber reinforced composites continue to steadily increase in absolute value. Therefore, the cooperativity plots of the composites are closer to linear in shape and cannot be reasonably fit to Eq. (2). At temperatures close to T_g all of the samples display nearly identical cooperativity. The curves begin to separate near $T_g + 20°C$, where $(T - T_g)/T_g \approx 0.04$, and can be distinguished at this point.

The effect of the fiber sizing becomes more pronounced at $T > T_g + 30°C$. This indicates that the viscoelastic behavior of the polymeric component of a composite material is more complicated and is altered by the presence of the fibers. The failure of Eq. (2) to fit to the composite data could be indicative of multiple over-lapping relaxation mechanisms occurring simultaneously within the matrix, sizing, and/or interphase region. If the fiber–matrix interphase, created through the inter-diffusion of the individual chemical species during fabrication, is restricted in mobility then the segmental relaxation of this region may occur at a higher temperature than the non-reinforced bulk matrix phase. The calculated values of n, based upon the E' data, have also been summarized in Table 2.

The shift factor data obtained from the E' master curves was also examined by plotting $\log a_T$ versus $1/T$ to give the Arrhenius activation energies (Fig. 9). All of the composite samples exhibit similar values of E_a at $T = T_g$ (Table 2). Each of the composite samples deviates from Arhennius

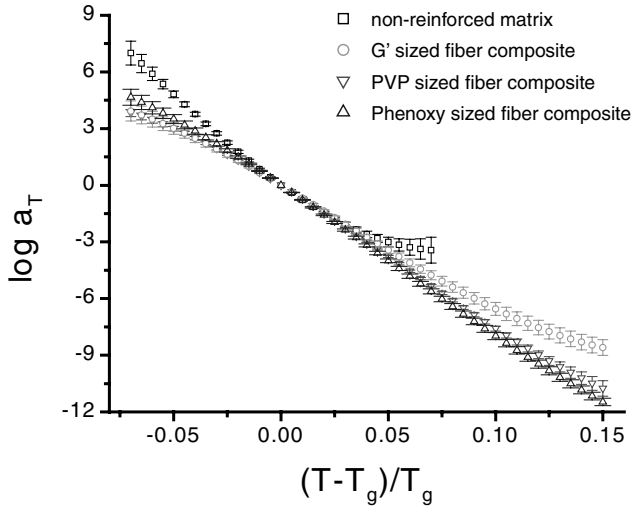

Fig. 7. Cooperativity plots at temperatures above and below T_g. Log a_T values taken from E' master curves.

behavior significantly at temperatures below T_g. The non-reinforced matrix has the highest activation energy at $T = T_g$. The non-reinforced matrix also displays the least amount of non-equilibrium behavior in the glassy state. The non-reinforced matrix would not be restricted in mobility by the glass fibers and should have less free volume upon cooling, at the same rate, leading to an increase in E_a. Sullivan et al. [19] determined that the viscoelastic relaxation times of E-glass composites seem to be universal in the glassy and short time regions near T_g. At temperatures much greater than T_g the non-reinforced matrix begins to deviate from Arhennius behavior while the composite samples continue to follow this relationship.

3.3. E'' master curves

The same molecular relaxation mechanism should be responsible for both E' and E'' modulus viscoelastic response observed in glass transition region of a polymer, as stated by the Kramers–Kronig relationship [24]. This relationship is followed for the case of the non-reinforced matrix. Fig. 10 shows the E'' master curve for the non-reinforced matrix plotted in the frequency domain. A comparison of the E' and E'' shift factors is shown in Fig. 11. The loss modulus relaxation spectrum of the non-reinforced matrix was described acceptably by the KWW equation by numerically solving the integral form of Eq. (1) [25,26]

$$E''(\omega) = \omega \int_0^\infty E(t) \cos(ax)\, dt \tag{6}$$

The KWW value of n yielded a value of 0.773 for the non-reinforced matrix in comparison to 0.510 as determined via the cooperativity analysis. A possible explanation for the discrepancy is in that the cooperativity method for solving n provides a very poor fit of experimental shift factor data measured below T_g, due to non-equilibrium glassy response. The KWW analysis is able to encompass the entire loss modulus spectrum near the glass transition of the polymer. However, the E' and E'' shift factors for the non-reinforced matrix were in excellent agreement, as shown in Fig. 11.

While time-temperature superposition of the composites appeared successful for the E' data, the results for the E'' data were not in very good agreement. Fig. 12 shows the loss modulus master curve for the G' pretreated fiber composite plotted in the frequency domain and the best-fit

Table 2
Coupling parameters and activation energies.

Sample	n	E_a (kJ/mol)
Non-reinforced matrix	0.510 (±0.014)	647 (±42)
G' sized fiber composite	0.649 (±0.219)	492 (±28)
PVP sized fiber composite	0.702 (±0.624)	532 (±22)
Phenoxy sized fiber composite	0.718 (±0.705)	574 (±27)

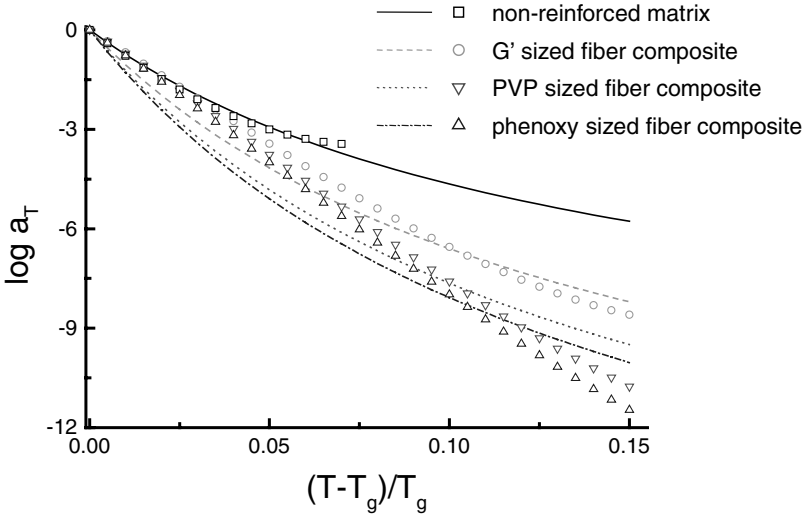

Fig. 8. Cooperativity plots at $T > T_g$ with best fit approximations of n using Eq. (2). Log a_T values taken from E' master curves.

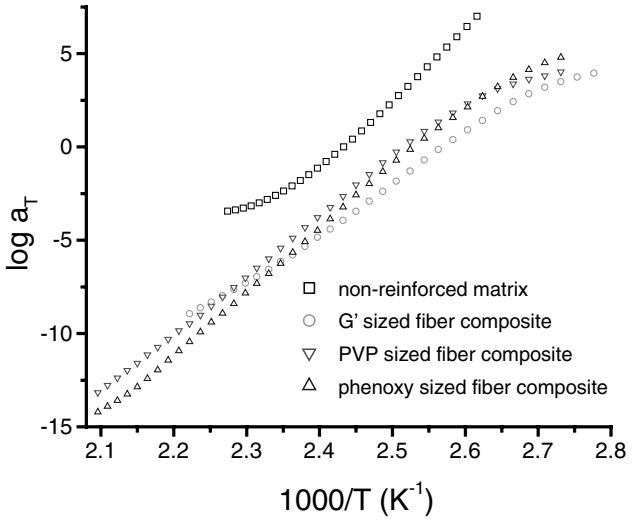

Fig. 9. Arrhenius activation energy plots taken from E' shift factor data.

to the KWW equation. Some anomalous behavior is observed in this plot and the fit to the KWW equation. At in the glassy state at high frequencies the theoretical KWW response is followed. At low frequencies the loss modulus spectrum for the G' pretreated fiber composite begins to deviate significantly from the KWW fit. The master curve of Fig. 12 should be compared to the corresponding E' and E'' shift factor plots illustrated in Fig. 13. The KWW expression is a flexible fitting function and can be forced to fit either the high or low frequency response of the composite, but not both simultaneously. The shift factor plots for the E' and E'' data are nearly identical for temperatures $T < T_g$. Time-temperature superpositioning of the loss modulus for the G' pretreated fiber composite is only successful in a small range of temperatures at $T > T_g$. Hence, the loss modulus cannot be shifted to the low frequencies as observed with the storage modulus for the G' pretreated fiber composite. Therefore, the shift factor data seems to indicate that the deviation from KWW response in the composite material is at the lower frequencies. Time-temperature superpositioning of the loss modulus for the

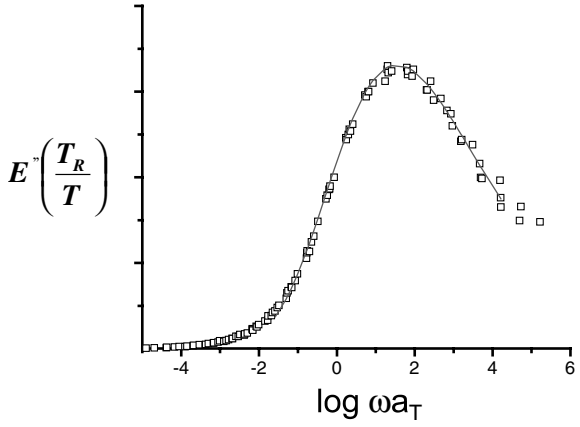

Fig. 10. Loss modulus master curve for non-reinforced matrix.

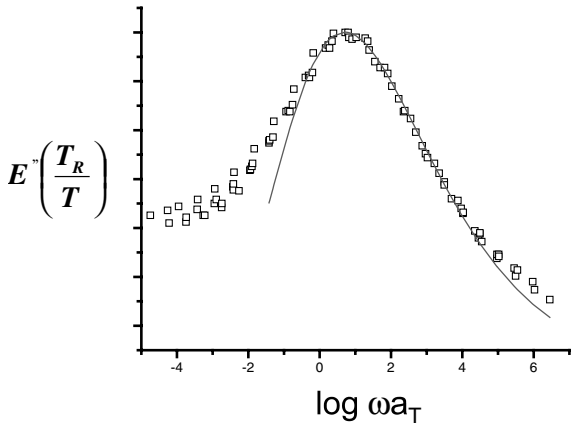

Fig. 11. Shift factors for non-reinforced matrix obtained from E' and E'' master curves.

PVP and Phenoxy sized fiber composites was completely unsuccessful at temperatures at $T > T_g$. Vertical shifting of the loss modulus curves for the composite samples was also investigated, but no trends were apparent. Sullivan et al. [19] observed that vertical shifting was required for time-temperature superposition in vinyl ester/E-glass composites. These researchers also found no clear trends with regard to the vertical shift factors for composite materials. The loss modulus may place more emphasis on certain portions of the relaxation spectra of the composite materials than the storage modulus.

3.4. Mechanical properties

Fig. 14 shows the quasi-static tensile strength for the individual composites. As it can be seen, the G' sizing did not perform as well as the Phenoxy and PVP sizings. Further, a relationship seems to connect the mechanical data, one which tends to be corroborated by the E' viscoelastic data shown in Fig. 8. It appears to that the composite with the greatest E' cooperativity tends to be the strongest in tension. The tensile modulus is depicted in Fig. 15. Fig. 16 shows the apparent shear strength obtained from short beam shear test data. An identical trend seems to exist as compared to the tensile strength data. The trends in the data seem to indicate that the process of fracture that tends to dominate in measurement of strength in a unidirectional composite can be influenced by the type of sizing polymer that is applied on the fiber. The interphase that develops via interdiffusion of the sizing polymer and the matrix resin indicates differences in terms of the composite's viscoelastic response, especially with respect to the packing features as it cools to form the glass. This is clearly depicted through the E' cooperativity results presented above. In this study, since carbon fiber was the only reinforcement used, the high temperature transition is possibly a reflection of the existence of an interphase region. Speculating, the resin at the interphase region could be highly constrained. In work done by Shan et al. [27] it was

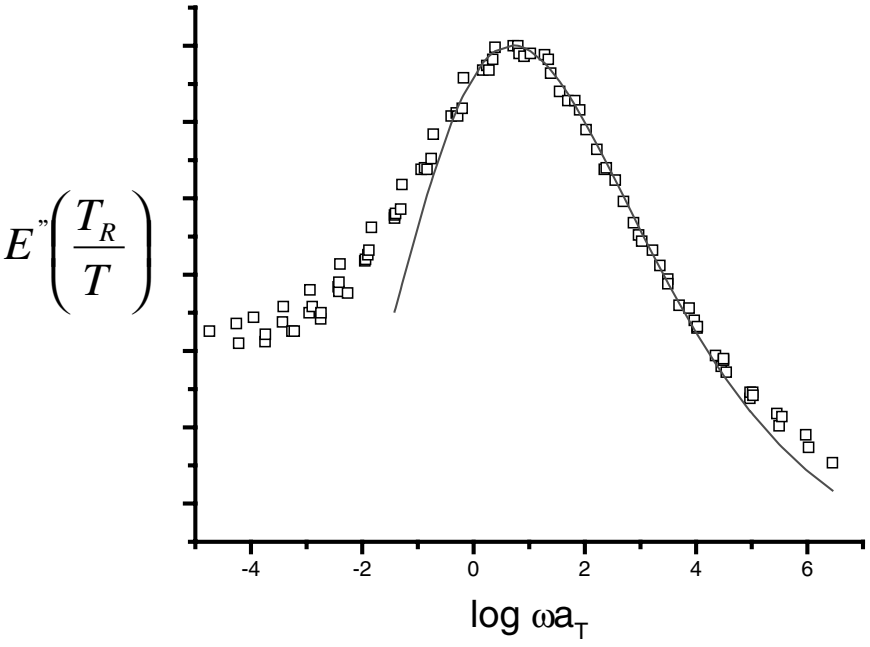

Fig. 12. Loss modulus master curve for G' fiber pretreated composite.

observed that the packing features dramatically influenced the fracture toughness of the polymer. Their study looked at the effect of network architecture on the viscoelastic behavior of vinyl ester resin. The effect of changing the molecular weight between crosslinks was clearly seen to influence the cooperativity or fragility analysis. Further, a strong correlation seemed to exist between the fracture toughness of the polymer and a normalized quantity that involved the cooperative domain size and the molecular weight between crosslinks. From this, it can be suggested that the increase in tensile strength of the composites was due to the increased fracture toughness at the interphase, an inference that was confirmed from the viscoelastic (cooperativity) studies. A similar observation has been made by Rosen [28] while trying to identify the mechanism of tensile failure in unidirectional composites. He describes the importance of having a tough matrix especially when the bonding to the fiber is good in order to prevent the propagation of the initial crack, across the composite causing premature failure. In addition to the above discussed mechanical properties, the interphase has also been reported to have a dramatic influence on the fatigue response (durability) of composites [21].

4. Conclusions

In the present paper the viscoelastic response has been explored for carbon fiber reinforced, unidirectional composites with different fiber sizings. Time-temperature superpositioning was successfully applied to the composite materials to construct master curves of the storage modulus in the frequency domain. The temperature dependence of the logarithmic shift factors, cooperativity, was found to vary with fiber sizing. Additionally, it was observed that the apparent cooperativity of the composite samples was always increased in comparison to the non-reinforced matrix. This is an expected result if the segmental relaxation process of the bulk matrix is retarded considerably due to additional constraints resulting from fiber–matrix or matrix–interphase interactions. This is the primary hypothesis of coupling theory, which states that the relaxation behavior of polymers is affected intermolecular interactions in addition to intramolecular coupling restrictions. Polymer chains that are more sterically restricted by neighboring chains tend to require a higher degree of cooperative motion to achieve segmental relaxation. London dispersion forces,

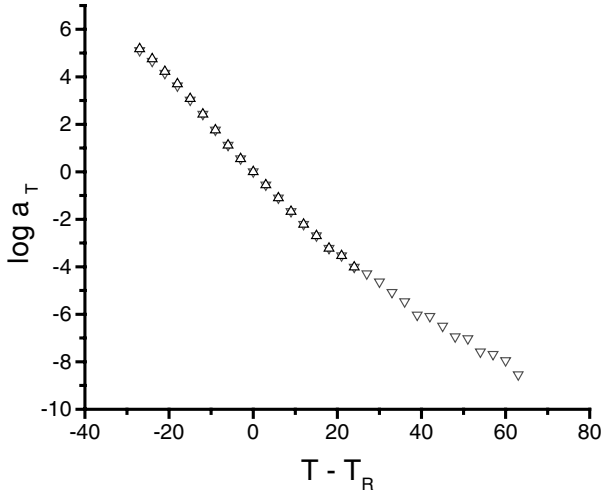

Fig. 13. Shift factors for G' fiber pretreated composite obtained from E' and E'' master curves.

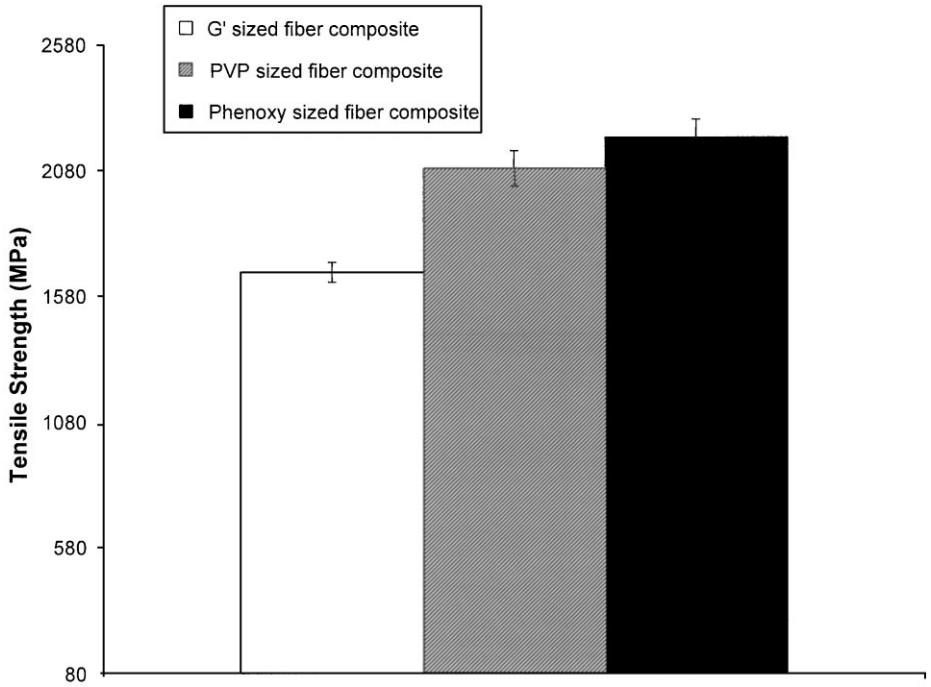

Fig. 14. Tensile strength of unidirectional carbon fiber–vinyl ester composites with different sizings.

hydrogen bonding, polar interactions, network formation, fillers etc. can all be included in this category of intermolecular restrictions.

This paper has investigated the sensitivity and applicability of cooperativity analysis of fiber reinforced composite materials in probing the viscoelastic response as a function of fiber sizing. The cooperativity of the composites, taken from storage modulus data, was clearly dependent on the sizing used to pretreat the fibers. The experimental cooperativity plots of the composite materials deviated significantly from theoretical predictions, but mechanical test data on these composites indicated a strong correlation between tensile strength and relaxation behavior. The Phenoxy sizing, which displayed the greatest temperature dependence

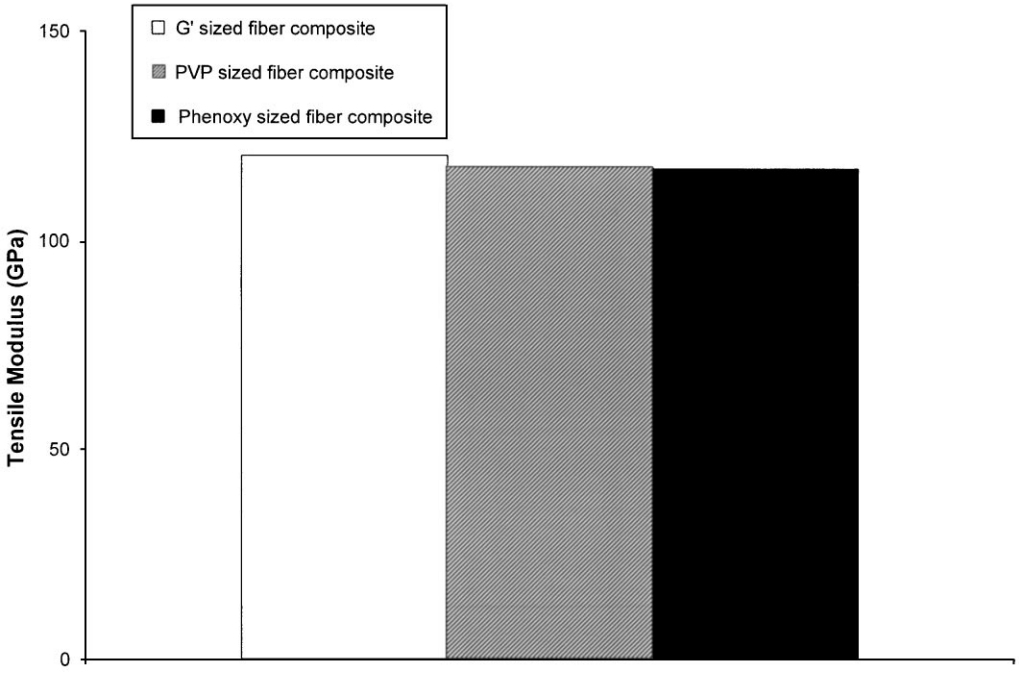

Fig. 15. Tensile modulus of unidirectional carbon fiber–vinyl ester composites with different sizings.

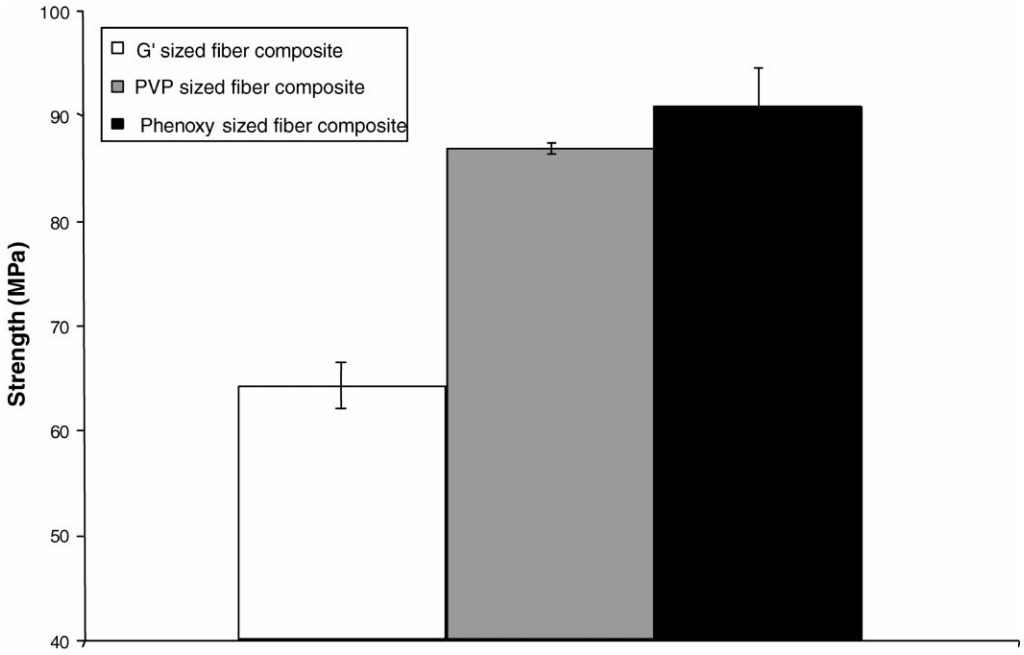

Fig. 16. Apparent shear strength of unidirectional carbon fiber–vinyl ester composites with different sizings.

of the logarithmic shift factors, exhibited the highest strength. The order for both tensile strength and apparent cooperativity are as follows, vinyl ester matrix $< G' <$ PVP $<$ Phenoxy. This possible connection between the viscoelastic behavior and both the fracture toughness and tensile strength of the composite was speculated to be due to similar origins. It is well known that strength is a fracture controlled process and so such a correlation may be likely. In the authors' view, the ability to draw qualitative connections between molecular behavior and specimen level macroscopic strength are invaluable especially considering the range of material structure that is covered and the possibility of using such a technique as a screening tool.

However, while a possible correlation between the mechanical and cooperative responses of composite materials was observed, our viscoelastic analysis leaves many unanswered questions. The main concern was our inability to duplicate the cooperativity analysis based on storage modulus data with loss modulus data. Time–temperature superposition of the loss modulus for the G' pretreated fiber composite could only be applied in a narrow frequency range at the glass transition. Time–temperature superposition of the loss modulus for the PVP and Phenoxy pretreated fiber composites was not possible at all. Similar irregular behavior, specifically the lack of agreement between shift factors, has been reported in stress relaxation and creep behavior for rubber-toughened epoxies [29]. These researchers proposed several possible explanations for this behavior including residual stresses, local non-linear viscoelastic response, as well the two phase nature of the rubber-toughened epoxy that was studied. Each of these explanations could certainly be applied in the case of our composite samples. The loss modulus plots of the PVP and Phenoxy pretreated fiber composites give evidence of a second phase, which could negate the use of a simple viscoelastic approach such as cooperativity analysis. It is hoped that these results provide insight to others investigating the viscoelastic and mechanical properties of composite materials.

Acknowledgements

The authors gratefully acknowledge support from the NSF Science and Technology Center for High Performance Polymeric Adhesives and Composites under contract number, DMR-9120004. Funding was also graciously provided by the Center for Adhesive and Sealant Science as well as the Adhesive and Sealant Council Education Foundation. The authors would like to thank Norman Broyles and Dr R.M. Davis in the Chemical Engineering Department at Virginia Tech for all their support. We would also like to thank Clint Smith at Strongwell (Bristol, Virginia) for time and assistance with the lab-scale pultruder.

References

[1] Madhukar MS, Drzal LT. J Comp Mater 1991;25:932.
[2] Madhukar MS, Drzal LT. J Comp Mater 1991;25:958.
[3] Madhukar MS, Drzal LT. J Comp Mater 1992;26:936.
[4] Lesko JJ, Swain RE, Cartwright JM, Chin JW, Reifsnider KL, Dillard DA, Wightman JP. J Adhes 1994;45:43.
[5] Lewis TB, Nielsen LEJ. Appl Polym Sci 1970;14:1449.
[6] Cousin P, Smith PJ. Polym Sci, Polym Phys 1994;32:459.

[7] Tsagaropoulos G, Eisenberg A. Macromolecules 1995;28:396.
[8] Tsagaropoulos G, Eisenberg A. Macromolecules 1995;28:6067.
[9] Reed KE. Polym Compos 1980;1:44.
[10] Thomason JL. Polym Compos 1990;11:105.
[11] Landel RF. Trans Soc Rheo 1958;2:53.
[12] Fitzgerald JJ, Landry CJT, Pochan JM. Macromolecules 1992;25:3715.
[13] Williams G, Watts DC. Trans Faraday Soc 1970;66:80.
[14] McCrum NG, Read BE, Williams G. Anelastic and dielectric effects in polymeric solids. New York: Dover, 1991.
[15] Plazek DJ, Ngai KL. Macromolecules 1991;24:1222.
[16] Roland CM, Ngai KL. Macromolecules 1991;24:5315.
[17] Roland CM, Ngai KL, O'Reilly JM, Sedita JS. Macromolecules 1992;25:3904.
[18] Jensen RE, O'Brien E, Wang J, Bryant J, Ward TC, James LT, Lewis DA. J Polym Sci, Polym Phys 1998;36:2781.
[19] Sullivan JC, Wen YF, Gibson RF. Polym Compos 1995;16:3.
[20] Buhler, Volker, Kollidon: Polyvinylpyrollidone for the Pharmaceutical Industry, BASF publication.
[21] Broyles NS, Verghese KNE, Davis SV, Li H, Davis RM, Lesko JJ, Riffle JS. Polymer 1998;39:3417.
[22] Broyles NS, Verghese KNE, Davis RM, Lesko JJ, Riffle JS. In preparation.
[23] Verghese KNE. PhD dissertation, Virginia Polytechnic Institute and State University, August 1999, http://scholar.lib.vt.edu/theses/available/etd-082799-151752/.
[24] Ferry JD. Viscoelastic properties of polymers. 2nd ed. New York: Wiley, 1970.
[25] Weiss GH, Bendler JT, Dishon MJ. Chem Phys 1985;83:1424.
[26] Weiss GH, Dishon M, Long AM, Bendler JT, Jones AA, Inglefield PT, Bandis A. Polymer 1994;35:1880.
[27] Shan L, Robertson CG, Verghese KNE, Burts E, Riffle JS, Ward TC, Reifsnider KL. Submitted for publication.
[28] Rosen BW. Chap. 3, vol. 37, American Society for Metals, Metals Park, 1965.
[29] Lee A, McKenna GBJ. Polym Sci, Polym Phys 1997;35:1167.